

UNCLASSIFIED

AD NUMBER

AD822660

LIMITATION CHANGES

TO:

Approved for public release; distribution is unlimited.

FROM:

Distribution authorized to U.S. Gov't. agencies and their contractors;
Administrative/Operational Use; 16 NOV 1967.
Other requests shall be referred to Space and Missile Systems Organization, Norton AFB, CA 92409.

AUTHORITY

SAMSO ltr 28 Feb 1972

THIS PAGE IS UNCLASSIFIED

88

AD 822660

AD 822660
FILE COPY

EXPERIMENTAL AND THEORETICAL KINETICS OF HIGH TEMPERATURE FLUOROCARBON CHEMISTRY

Prepared by

AVCO MISSILES, SPACE AND ELECTRONICS GROUP
MISSILE AND SPACE SYSTEMS DIVISION
AEROPHYSICS LABORATORY
201 Lowell Street
Wilmington, Massachusetts 01887

AVMSD-0734-67-CR
Contract F04(694)-67-C-0060 and
Contract DA-01-021-AMC 12005 (Z)
CDRL Item 6

November 16, 1967

DDC
RECEIVED
NOV 20 1967
RECEIVED

B

THIS DOCUMENT IS SUBJECT TO SPECIAL EXPORT CONTROLS AND EACH TRANSMITTAL TO FOREIGN GOVERNMENTS OR FOREIGN NATIONALS MAY BE MADE ONLY WITH PRIOR APPROVAL OF SPACE AND MISSILE SYSTEMS ORGANIZATION (SMSO).

Prepared jointly for

ADVANCED RESEARCH PROJECTS AGENCY

Monitored by the
ARMY MISSILE COMMAND
UNITED STATES ARMY
Redstone Arsenal, Alabama

SPACE AND MISSILE SYSTEMS ORGANIZATION
DEPUTY FOR REENTRY SYSTEMS
AIR FORCE SYSTEMS COMMAND
Norton Air Force Base, California 92409

FOR OFFICIAL USE ONLY

18
19
SAMSD-TR-67-20
6

9 Technical Rept.

This document consists of 33 pages,
87 copies, Series A

**EXPERIMENTAL AND THEORETICAL KINETICS OF
HIGH TEMPERATURE FLUOROCARBON CHEMISTRY.**

Prepared by

AVCO MISSILES, SPACE AND ELECTRONICS GROUP
MISSILE AND SPACE SYSTEMS DIVISION
~~AEROPHYSICS LABORATORY~~
201 Lowell Street
Wilmington, Massachusetts 01887

15
14 AVMSD-0734-67-CR
~~FO4694-67-C-0060~~
FO4694-67-C-0060, DA-01-021-AMC 12005(Z)
CDRL Item 6
11/16 Nov 1967 12 33p.

by

10 Anthony P. Modica
APPROVED

G. Luceri
G. Luceri, Manager
REST Program

THIS DOCUMENT IS SUBJECT TO SPECIAL EXPORT CONTROLS AND
EACH TRANSMITTAL TO FOREIGN GOVERNMENTS OR FOREIGN
NATIONALS MAY BE MADE ONLY WITH PRIOR APPROVAL OF SPACE
AND MISSILE SYSTEMS ORGANIZATION (SMSD).

Prepared jointly for

ADVANCED RESEARCH PROJECTS AGENCY

Monitored by the
ARMY MISSILE COMMAND
UNITED STATES ARMY
Redstone Arsenal, Alabama

SPACE AND MISSILE SYSTEMS ORGANIZATION
DEPUTY FOR REENTRY SYSTEMS
AIR FORCE SYSTEMS COMMAND
Norton Air Force Base, California 92409

mt

402 572

1473
elk

ABSTRACT

Ultraviolet absorption was used to measure the rate of formation of difluoromethylene (CF_2) from decomposed CF_3I , C_2F_6 , and CF_4 in excess argon behind shock waves. In some experiments pure CF_4 was shocked. Data were taken over a temperature range from 1700° to 3000° K at total concentrations between $2(10^{-5})$ and $5(10^{-6})$ mole- cm^{-3} . A chemical, nonequilibrium shock-tube computer program was developed to analyze the CF_2 kinetic profiles. By curve fitting the data, rate constants for a number of fluorocarbon reactions are obtained.

Unclassified report

A copy of this report is available at Reports Distribution Center, Room 1126 and will be held for a period of three weeks.

EDITED BY:
EDITORIAL SERVICES SECTION
P. S. Falcey

Foreword

This report presents work performed by the Chemical Physics Research Group of the Aerophysics Laboratory of the Avco Corporation Missile and Space Systems Division, 201 Lowell Street, Wilmington, Massachusetts. The present task has been supported jointly by the Space and Missile Systems Organization (SAMSO), Deputy for Ballistic Missile Reentry Systems, Air Force Systems Command, Norton Air Force Base, California, under Contract FO4 (694)-67-0060 part of the ABRES Program; and by the Avco Everett Research Laboratory (AERL) for the Advanced Research Projects Agency (ARPA), monitored by the Army Missile Command, United States Army, Redstone Arsenal, Alabama, under Contract No. DA-01-021 AMC-12005 (Z), part of the Project DEFENDER.

Information in this report is embargoed under the Department of State to foreign governments by department or agencies of the U.S. Government subject to approval of Space and Missile Systems Organization (SMSO), Norton Air Force Base, California, or higher authority within the Department of the Air Force. Private individuals or firms require a Department of State export license.

The Air Force monitor for the ABRES REST Program is Capt. W. Mercer, SMYSE, USAF, Project Officer.

This technical report has been reviewed and is approved.

Capt. W. Mercer, SMYSE
REST Project Office
Space and Missile System Organization
Norton Air Force Base, California

CONTENTS

I.	Introduction	1
II.	Experimental Measurements	2
III.	Nonequilibrium Shock Tube Program	3
IV.	Chemical Mechanisms and Kinetics	5
V.	Discussion	7
VI.	References	9
VII.	Appendix A: Formulation of the Nonequilibrium Shock-Tube Program	10

ILLUSTRATIONS

Figure 1	Difluoromethylene Ultraviolet Light Absorption Behind Shock Waves	18
2	Numerical Check of Nonequilibrium Shock-Tube Program with Airchemistry Stream-Tube Calculation	19
3	Chemical Kinetics Shock-Tube Calculation for Decomposition of 1:100 CF_3I - Argon Gas Mixture	20
4	Chemical Kinetics Shock-Tube Calculation for Decomposition of 1:100 C_2F_6 - Argon Gas Mixture	21
5	Experimental Rate Constant for CF_3 Dissociation	22
6	Chemical Kinetics Shock-Tube Calculation for Decomposition of 1:100 CF_4 - Argon Gas Mixture	23
7	Experimental Rate Constant for CF_4 Dissociation	24
8	Chemical Kinetics Shock-Tube Calculation for Decomposition of Pure CF_4	25
9	Kinetic Profiles of CF_4 in Shock Heated Fluorocarbon-Argon Gas Mixtures	26

TABLES

Table 1	Fluorocarbon Reactions and Rate Constants	15
2	Examples of CF_3I and C_2F_6 Shock Tube Experiments	16
3	Examples of CF_4 Shock Tube Experiments	17

INTRODUCTION

The role of fluorine in the high temperature oxidation chemistry of tetrafluoroethylene (C_2F_4) is little understood. For example, among the reaction products of C_2F_4 and its polymer with oxygen, there have been identified CF_4 and CF_3 species. (1,2) It was suspected that these molecules resulted from the reaction between fluorine and the difluoromethylene radical (CF_2). Support of this hypothesis was noted when shock heated mixtures of CF_3I , C_2F_6 and CF_4 in argon diluent as well as pure CF_4 were found to decompose to CF_2 . Experiments were carried out to detect the CF_2 radical by its absorption in the ultraviolet. In the present paper, measured kinetic profiles of this species are analyzed with a computer program. The computer program solves simultaneously the Hugoniot relations (mass, momentum, and energy) and the chemical rate equations for a chemically unrelaxed shock wave. The calculated rate profiles of CF_2 are compared with experiment. Some of the rate constants employed in the analysis were taken from literature sources, some were determined empirically and others were estimated from theory or deduced from JANAF equilibrium constants.

EXPERIMENTAL MEASUREMENTS

The shock-tube apparatus has been described previously.⁽¹⁾ It consists of 1.5-inch inside diameter stainless steel sections provided with light screens for shock velocity measurements and an optical station for ultraviolet absorption spectroscopy. Gas mixtures of CF_4 (Matheson, 95 percent purity), CF_3I (Air Products, 98 percent purity), C_2F_6 (Air Products, 99.9 percent) in excess argon (Matheson, 99.999 percent purity) were prepared for study. A few tests were conducted in undiluted CF_4 . The CF_2 radicals in the shock-heated reaction mixtures were followed photometrically in absorption at 2660\AA . The absorption coefficient, 1.15×10^6 (± 10 percent) cubic centimeter per mole-centimeter, was used to calculate concentration from Beer's law.⁽³⁾ Oscillogram records shown in Figure 1 are typical of the CF_2 absorption from these gas mixtures. The CF_3I and C_2F_6 molecules were studied since CF_3 radicals are immediately formed behind the shock wave, making the rate determining step for CF_2 appearance the dissociation of CF_3 . With CF_4 , the complete fluorocarbon chemistry involving CF_4 , CF_3 and CF_2 is given. By studying the decomposition rates leading to CF_2 , the kinetics of the fluorine oxidation reactions may thus be ascertained from detail balancing with appropriate equilibrium constants.

NONEQUILIBRIUM SHOCK TUBE PROGRAM

The equations governing a moving one-dimensional inviscid fluid in a shock tube are the so-called Rankine-Hugoniot⁽⁴⁾ relations expressing conservation of mass, momentum, and energy,

$$d(\rho u)/dt = 0 \quad (\text{mass}) \quad (1)$$

$$\rho u d\left(u + \frac{p}{\rho u}\right)/dt = 0 \quad (\text{momentum}) \quad (2)$$

$$\rho u d\left(h + \frac{1}{2} u^2\right)/dt = 0 \quad (\text{energy}) \quad (3)$$

where ρ is the density, u is the flow velocity, p is pressure and h is the enthalpy per unit mass. For a multi-component gas h is defined by

$$h = \frac{\sum c_i h_i}{\sum c_i M_i} \quad (4)$$

The quantity c_i is the concentration of the i^{th} species in mole per cubic centimeter, h_i is the molar enthalpy and M_i the gram molecular weight. The ideal gas equation

$$p = \frac{\rho \sum c_i}{\sum c_i M_i} RT \quad (5)$$

is used to relate the thermodynamic temperature T to pressure and density where R is the universal gas constant per mole. The molar enthalpy is then expressed in terms of temperature by a power series,

$$h_i = \left(L_1 T + \frac{L_2 T^2}{2} + \frac{L_3 T^3}{3} + \frac{L_4 T^4}{4} - L_5 T^{-1} + L_6 \right)_i \quad (6)$$

A curve fit of the molar enthalpy of each species was generated from JANAF thermochemical data.⁽⁵⁾ The variation in species concentration resulting from chemical reaction and volumetric change behind the shock wave is given by

$$\begin{aligned} \frac{dc_i}{dt} - \frac{c_i}{\rho} \frac{d\rho}{dt} &= \sum \pi \nu_{kj} c_k A_{fj} T^{n_j} \exp(E_{fj}/RT) \\ &- \sum \pi \nu_{ij} c_i A_{rj} T^{n_j} \exp(E_{rj}/RT) \end{aligned} \quad (7)$$

where the positive term on the right of the equality reflects the sum of the chemical rates leading to species production and the negative term, the rates for removal. Subscripts f and r denote the forward and reverse processes, ν_{kj} and ν_{ij} are the stoichiometric coefficients for the k^{th} and i^{th} species in the j^{th} reaction; A_j , n_j and E_j are the pre-exponential factor, temperature exponent, and activation energy of the rate constant for that reaction. To solve this set of differential equations for a multicomponent, chemically relaxing shock wave, a Runge-Kutta integration scheme⁽⁶⁾ and an IBM 360 computer were employed. The inputs to the calculation are the shock velocity, state of the gas ahead of the shock wave, the chemical reactions to be considered, the forward and reverse rate constants, and coefficients of the enthalpy curve-fits. Typical machine times for solving the fluorocarbon chemical kinetics problems ran between 1 and 2 minutes. Before using the nonequilibrium shock-tube program to analyze the present data, a program check was made against an air chemistry, stream tube program developed by M. G. Mamin and O'Brien.⁽⁷⁾ Figure 2 shows that calculations from both programs for electron density behind a shock wave into air agree numerically to within 3 percent.

CHEMICAL MECHANISMS AND KINETICS

The reactions considered in this study are shown in Table 1.

CF₃I and C₂F₆ Decomposition: A bimolecular rate constant for R1 was estimated from classical collision theory⁽⁸⁾ assuming energy contributions from half the number of vibrational modes and a steric factor of 0.1. The dissociation rate constant of R2 was obtained from the JANAF equilibrium constant and the rate constant of Ayscough⁽⁹⁾ for trifluoromethyl radical recombination. Calculations based on these rate constants (Figures 3 and 4) showed that within a few microseconds after shock passage CF₃I was dissociated by several orders of magnitude and that C₂F₄ was about 80 percent dissociated with R2 and R2' in equilibrium. Under these conditions, the apparent rate constant for CF₂ formation by CF₃ dissociation (R3) is given by

$$\frac{d[CF_2]}{\rho_{21} dt} = k_3 (\text{expt}'1) \{ [CF_3]_0 - (1 + \gamma) [CF_2] \} [Ar] \quad (8)$$

where γ is zero if $R4' \ll R3$ and one if $R4' \gg R3$, i.e., for each CF₂ produced one CF₃ radical is removed when fluorine attachment is slow and two CF₃ radicals are removed when fluorine attachment is fast. The concentration of CF₃ initially behind the shock wave is $[CF_3]_0$. The density ratio ρ_{21} is multiplied in Equation (8) to reference the event to laboratory time (t_l). In calculating k_3 (expt'1) by means of Equation (8), γ was taken to be unity for the lower temperature data, and was assumed zero for the higher temperature data. Calculations (Figures 3 and 4) indicated that when analyzing the low temperature data after 50 percent decomposition, the above approximation was good to within 90 percent. Another feature brought out by the calculations was that after CF₃I and C₂F₆ chemical relaxation, the shock temperature profile was nearly constant, so that little temperature uncertainty was introduced in evaluating the rate constant for R3 during reaction. With the higher temperature data, k_3 (expt'1) was determined from the initial CF₂ absorption slope. As seen in Figure 5, the rather good agreement obtained within the scatter limits of k_3 (expt'1) in the CF₃I and C₂F₆ experiments tends to uphold the data reduction method. Examples of the CF₃I and C₂F₆ study are given in Table 2.

CF₄ Decomposition: In the temperature range 2200° to 3000° K, the CF₃ dissociation rate is three orders of magnitude faster than the rate of appearance of CF₂ in the oscillogram records of CF₄ decomposition. Hence these observations suggested that the rate determining step for CF₂ formation starting with CF₄ was R4. Calculations (Figure 6) showed that under the experimental conditions chosen the CF₃ concentration would be much less than that of CF₂ and CF₄ in the reaction mixture, allowing an apparent rate constant for R4 to be evaluated from the initial CF₂ slope measurements according to

$$\frac{d[CF_2]}{\rho_{21} dt} = k_4 (\text{expt}'1) \{ [CF_4]_0 - [CF_2] \} [Ar]. \quad (9)$$

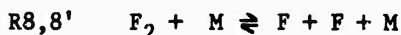
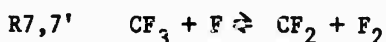
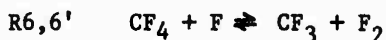
Examples of the experiments are shown in Table 3. The temperature dependence of the apparent rate constants obtained from 1:100 and 2:100 CF_4 -Argon gas mixtures is shown in Figure 7. The kinetic profile of CF_2 measured in a pure CF_4 run (Figure 8) is compared to that calculated from the nonequilibrium shocktube program using the rate constants in Table 1. The results indicate that the collision efficiencies of CF_4 and argon appear to be quite similar. Another aspect of the pure CF_4 experiment is that the intermediate CF_3 chemistry becomes important and serves as a check on its rate constants in the calculations. The rate constants for R5 and R5' were obtained in an earlier study of the thermal decomposition of the difluoromethylene radical⁽¹⁰⁾.

Finally, for a number of shock conditions, measured and calculated kinetic profiles of CF_2 from decomposition of the three fluorocarbon molecules investigated are shown in Figure 9. It is seen that the rate constants given in Table 1 would appear to be adequate in describing the experimental data over the temperature range of the study.

DISCUSSION

The heat-of-reaction for R3 was obtained from JANAF thermochemical data and used to fit the experimental rate constants of the CF_3I and C_2F_6 data. The large temperature exponent ($T^{-9.04}$) determined appears to be inconsistent with the classical collision treatment for a polyatomic like CF_3 . The maximum number of internal degrees of freedom not counting rotations which could contribute energy for reaction would be 6. Rotational and translational participation, if included, would increase the temperature exponent to only ($T^{-8.5}$). It was found that in calculating the CF_2 rate profiles, good agreement with the measurements could be obtained with the JANAF equilibrium constant multiplied by 16. With the equilibrium pre-exponential factor kept constant, a factor of 16 gives a heat-of-reaction of 81.2 kcal/mole at 2000° K (average temperature range of data). By refitting the rate constants of R3 with the revised heat-of-reaction, a temperature exponent of ($T^{-6.21}$) is obtained, which is more in accord with theory.

Besides the reactions shown in Table 1, the rate data were also analyzed by adding the reactions



Calculations based on rate constants from classical collision theory and JANAF equilibrium constants showed that R6,6' and R7,7' were about three orders of magnitude slower than the decomposition reactions and had negligible effect on the measured CF_2 kinetic profiles.

ACKNOWLEDGEMENTS

The support of the Space and Missile Systems Organization/U. S. Air Force under Contract F04(694)-67-C-0060, part of ABRES Program, is gratefully acknowledged. The authors express thanks to Ronald Brochu for assisting in the collection and reduction of the shock-tube data.

REFERENCES

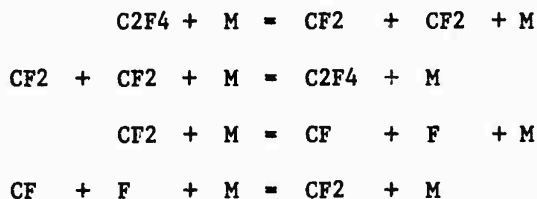
1. Modica, A. P. and J. E. LaGraff, "Decomposition and Oxidation of C_2F_4 Behind Shock Waves," *J. Chem. Phys.* 43, 3383 (1965).
2. Kupel, R. E., M. Nolan, R. G. Keenan, M. Hite and L. D. Scheel, "Mass Spectrometric Identification of Decomposition Products of Polytetrafluoroethylene and Polyfluoreoethylenepropylene," *Anal. Chem.* 36, 386 (1964).
3. Modica, A. P., "Electronic Oscillator Strength of CF_2 ," Avco Report AVMSD-0346-67-CR, (May 1967).
4. Courant, R. and K. O. Friedrichs, Supersonic Flow and Shock Waves (Interscience Publishers, Inc., New York, 1948).
5. JANAF Thermochemical Tables (Dow Chemical Co., Midland, Mich. 1961-1966).
6. Ralston, A. and H. S. Wilf, "Mathematical Methods for Digital Computers" (John Wiley and Sons, Inc., New York, 1964).
7. McMenamin, D. and M. O'Brien, "The Finite Difference Solution of Multi-component Nonequilibrium Steady Inviscid Streamtube Flows Using a Novel Stepping Technique. Part I Analysis and Applications," General Electric Co. Report 67SD241 (April 1967).
8. Fowler, R. and E. A. Guggenheim, Statistical Thermodynamics (Cambridge University Press, Cambridge, England, 1956).
9. Ayscough, P. B., "Rate of Recombination of Radicals. II. The Rate of Recombination of Trifluoromethyl Radicals," *J. Chem. Phys.* 24, 944 (1956).
10. Modica, A. P., "Kinetics and Equilibria of the Difluorocarbene Radical Decomposition Behind Shock Waves," *J. Chem. Phys.* 44, 1585 (1966).

APPENDIX A

Formulation of the Nonequilibrium Shock-Tube Program

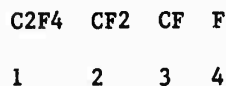
The nonequilibrium shock tube program solves simultaneously the Rankine-Hugoniot conservation relations and the chemical rate equations expressing variation in species concentration. The program is organized to integrate the rate equations stepwise, an iteration scheme to satisfy the conservation relations being repeated at each step. It differs from the average ordinary differential equation program chiefly in that the equations themselves are not fixed. Instead, only rules for generating the equations are fixed.

The input quantities include the shock velocity; the temperature, pressure, and species mole fractions ahead of the shock; the chemical reactions to be considered; the preexponential factor, temperature exponent, and activation energy of the rate constant for each reaction; and coefficients of the enthalpy curve fits. A library tape of species data (molecular weights and enthalpy fit coefficients) may be searched for quantities omitted from the regular program input. The chemical reactions are entered directly in equation form, a maximum of four species allowed on each side of an equation, with each species allotted a maximum of eight alphanumeric characters. For example, consider the simple system



where M will be taken by convention to refer to the sum of all species concentrations.

The set of equations is analyzed by the program, the species in each equation matched against an input list of all species occurring in the problem, and a matrix M of indices set up to represent the original equations. If, in the example above, the species are arbitrarily ordered,



and M is assigned the index 5, the 4x8 matrix generated by the program is

$$M = \left[\begin{array}{cccc|cccc} 1 & 5 & 0 & 0 & 2 & 2 & 5 & 0 \\ 2 & 2 & 5 & 0 & 1 & 5 & 0 & 0 \\ 2 & 5 & 0 & 0 & 3 & 4 & 5 & 0 \\ 3 & 4 & 5 & 0 & 2 & 5 & 0 & 0 \end{array} \right]$$

The rules for generating the set of differential equations are then as follows:

For the i^{th} species the change in the concentration $C_i(t)$ as a function of time is defined as

$$\frac{d}{dt} C_i(t) = \sum_{j=1}^{N_R} R_j (\delta_{l_j} + \delta_{r_j}) \prod_{K=1}^4 C_{M_j, K} \quad i = 1, \dots, N_S$$

where

N_S is the number of species

N_R is the number of reactions

R_j is the rate constant corresponding to the j^{th} equation

$$\delta_{l_j} = \begin{cases} -n & \text{if the } i^{\text{th}} \text{ species occurs } n \text{ times on the left} \\ & \text{side of equation } j \\ 0 & \text{if the } i^{\text{th}} \text{ species does not occur on the left} \\ & \text{side of equation } j \end{cases}$$

$$\delta_{r_j} = \begin{cases} +n & \text{if the } i^{\text{th}} \text{ species occurs } n \text{ times on the right} \\ & \text{side of equation } j \\ 0 & \text{if the } i^{\text{th}} \text{ species does not occur on the right} \\ & \text{side of equation } j \end{cases}$$

and by definition

$$C_0 = 1$$

$$C_{N_S+1} = \sum_{i=1}^{N_S} C_i$$

Again, for the example, the equations are

$$\frac{d}{dt} C_1 = (-R_1 C_1 + R_2 C_2^2) \sum_{i=1}^4 C_i$$

$$\frac{d}{dt} C_2 = (2 R_1 C_1 - 2 R_2 C_2^2 - R_3 C_2 + R_4 C_3 C_4) \sum_{i=1}^4 C_i$$

$$\frac{d}{dt} C_3 = (R_3 C_2 - R_4 C_3 C_4) \sum_{i=1}^4 C_i$$

$$\frac{d}{dt} C_4 = (R_3 C_2 - R_4 C_3 C_4) \sum_{i=1}^4 C_i$$

To find initial conditions for the system of differential equations, the conservation relations are first solved for values of the temperature $T_2(0)$ and density $\rho_2(0)$. A false position iteration for temperature is used in the solution. Then, since the mole fractions $X_i(t)$ are known (input) quantities at time 0, the concentrations can be found from the relation

$$C_i(t) = \frac{X_i(t) \rho_2(t)}{\sum_{i=1}^{N_S} X_i(t) M_i} \quad i = 1, \dots, N_S$$

where M_i is the molecular weight of the i^{th} species.

To solve the differential equations a fourth order predictor-corrector method, sometimes called the Modified Adams-Bashforth Method, is used. This method is generally available for computer use in an Avco library subroutine which was partially reprogrammed for purposes of the problem. The technique is particularly attractive because of its computational efficiency and the relative ease it affords in maintaining accuracy requirements. The one major disadvantage is that it is not self-starting.

Before the predictor-corrector algorithm can even be applied, values of all the concentrations $C_i(t)$, $i = 1, \dots, N_S$ and of their first derivatives $\frac{d}{dt} C_i(t)$, $i = 1, \dots, N_S$

must be known at each of four points in time. Information at the first point $t_0 = 0$ can be obtained directly from the initial conditions. Values at three additional equally-spaced points t_1 , t_2 , and t_3 are obtained by a fourth order Runge-Kutta integration process, the interval Δt between the points being controlled by program input. Runge-Kutta is particularly appropriate as a starting method since results at each step depend only on conditions at the last previous step. In addition, a high degree of accuracy can be established with a sufficiently small interval. (However, Runge-Kutta would present serious disadvantages if used over the entire time period. A relatively large number of derivative

calculations are required, and no immediate estimate of the truncation error is available.) In the fourth order Runge-Kutta method the derivatives are evaluated at four points in the interval and weighted to give agreement with a Taylor Series expansion through the fourth order term. For a comprehensive discussion of Runge-Kutta integration see chapter 9 in Mathematical Methods for Digital Computers, edited by Ralston and Wilf(6).

Given the starting values obtained from Runge-Kutta, the predictor-corrector algorithm operates as follows. For each concentration $C_i, i = 1, \dots, N_s$, a third degree polynomial $\tilde{P}_i(t)$ approximating $d/dt C_i$ is fitted through the four available derivative values. This polynomial is then integrated to give an extrapolated or predicted concentration

$$\tilde{C}_i(t_4) = C_i(t_3) + \int_{t_3}^{t_4} \tilde{P}_i(t) dt \quad i = 1, \dots, N_s$$

at $t_4 = t_3 + \Delta t$. From the set $\tilde{C}_i(t_4), i = 1, \dots, N_s$ approximate derivatives $d/dt \tilde{C}_i(t_4)$ are calculated directly. Then a new polynomial $\bar{P}_i(t)$ is fitted through $d/dt C_i(t_1)$, $d/dt C_i(t_2)$, and $d/dt C_i(t_3)$, and $d/dt \tilde{C}_i(t_4)$, and interpolated or corrected concentrations

$$\bar{C}_i(t_4) = C_i(t_3) + \int_{t_3}^{t_4} \bar{P}_i(t) dt \quad i = 1, \dots, N_s$$

are computed.

Since the truncation errors for the extrapolation and interpolation formulas are of the same order, the difference $C_i(t_4) - \tilde{C}_i(t_4)$ provides an estimate of the actual truncation error incurred by the integration scheme in the interval from t_3 to t_4 . In fact, it can be shown that, neglecting higher order terms, the true value $C_i(t_4)$ lies between $\bar{C}_i(t_4)$ and $\tilde{C}_i(t_4)$. Again, see reference (6), chapter 8 for a general discussion of predictor-corrector techniques.

In the algorithm the quantity $|\bar{C}_i(t_4) - \tilde{C}_i(t_4)|$ is tested to ensure that the integration is sufficiently accurate. A relative tolerance specified through program input, multiplied by $\sum_{i=1}^{N_s} C_i(0)$, is taken as an absolute upper limit for

$|\bar{C}_i(t_4) - \tilde{C}_i(t_4)|$. If for any i this limit is exceeded, the time interval Δt is halved and the integration retried. The process of testing, cutting the interval, and reapplying the predictor-corrector step is repeated until $|\bar{C}_i(t_4) - \tilde{C}_i(t_4)|$ is sufficiently small. Then the predicted values $\tilde{C}_i(t_4), i = 1, \dots, N_s$ are taken as the result of integration, and $d/dt \tilde{C}_i(t_4), i = 1, \dots, N_s$ as the set of corresponding derivatives. (The predicted rather than the corrected results are accepted to avoid computing the additional set of derivatives.) If, for each $i, |\bar{C}_i(t_4) - \tilde{C}_i(t_4)|$ is at least one hundred times smaller than the limiting criterion, the

interval Δt will be doubled before the next integration step is begun. The whole process is then repeated over successive intervals, at each step the latest Δt and conditions at the last four points entering the computation, until the end of the time period is reached.

The program was coded in FORTRAN IV for use on the IBM 360 series of computers. Execution times for typical problems on the 360 model 75 computer range between one and two minutes.

TABLE I
FLUOROCARBON REACTIONS AND RATE CONSTANTS^a

R1	$\text{CF}_3\text{I} + \text{M} \rightarrow \text{CF}_3 + \text{I} + \text{M}$	$k_1 = 2.27 \times 10^{30} T^{-4.0} \exp(-57385/RT)$
R2	$\text{C}_2\text{F}_6 + \text{M} \rightarrow \text{CF}_3 + \text{CF}_3 + \text{M}$	$k_2 = 8.40 \times 10^{20} T^{0.5} \exp(-76500/RT)$
R2'	$\text{CF}_3 + \text{CF}_3 + \text{M} \rightarrow \text{C}_2\text{F}_6 + \text{M}$	$k_2' = 7.14 \times 10^{17} T^{0.5}$
R3	$\text{CF}_3 + \text{M} \rightarrow \text{CF}_2 + \text{F} + \text{M}$	$k_3 = 1.57 \times 10^{49} T^{-9.04} \exp(-92254/RT)$
R3'	$\text{CF}_2 + \text{F} + \text{M} \rightarrow \text{CF}_3 + \text{M}$	$k_3' = 1.49 \times 10^{46} T^{-9.04} \exp(-2287/RT)$
R4	$\text{CF}_4 + \text{M} \rightarrow \text{CF}_3 + \text{F} + \text{M}$	$k_4 = 6.15 \times 10^{34} T^{-4.64} \exp(-122421/RT)$
R4'	$\text{CF}_3 + \text{F} + \text{M} \rightarrow \text{CF}_4 + \text{M}$	$k_4' = 9.79 \times 10^{31} T^{-4.64} \exp(-2849/RT)$
R5	$\text{CF}_2 + \text{M} \rightarrow \text{CF} + \text{F} + \text{M}$	$k_5 = 4.20 \times 10^{26} T^{-2.85} \exp(-106000/RT)$
R5'	$\text{CF} + \text{F} + \text{M} \rightarrow \text{CF}_2 + \text{M}$	$k_5' = 6.57 \times 10^{26} T^{-2.85}$
M = collision partner (Argon)		

^aunits in calories, cubic centimeter, degree Kelvin, mole, second.

TABLE 2
EXAMPLES OF CF₃I AND C₂F₆ SHOCK TUBE EXPERIMENTS

Experiment No.	Shock Velocity (mm/ μ sec)	^a Shock Temp. ($^{\circ}$ K)	<i>P</i> ₂₁	Total Gas Conc'n (mole/cm ³) 10 ⁶	Apparent Rate Constant (k ₃ , cm ³ /mole sec)
1:100 CF ₃ I - Argon Data					
1	1.322	1804	3.66	7.94	2.28 x 10 ⁸
2	1.382	1928	3.75	8.16	9.08 x 10 ⁸
3	1.441	2060	3.82	8.33	4.95 x 10 ⁹
4	1.478	2143	3.87	8.45	5.08 x 10 ⁹
5	1.510	2214	3.92	8.56	7.73 x 10 ⁹
1:100 C ₂ F ₆ - Argon Data					
6	1.347	1735	4.00	10.8	9.09 x 10 ⁷
7	1.395	1850	4.02	8.72	5.69 x 10 ⁸
8	1.440	1960	4.03	8.76	1.20 x 10 ⁹
9	1.456	2000	4.04	8.76	1.38 x 10 ⁹
10	1.533	2205	4.06	8.82	4.88 x 10 ⁹

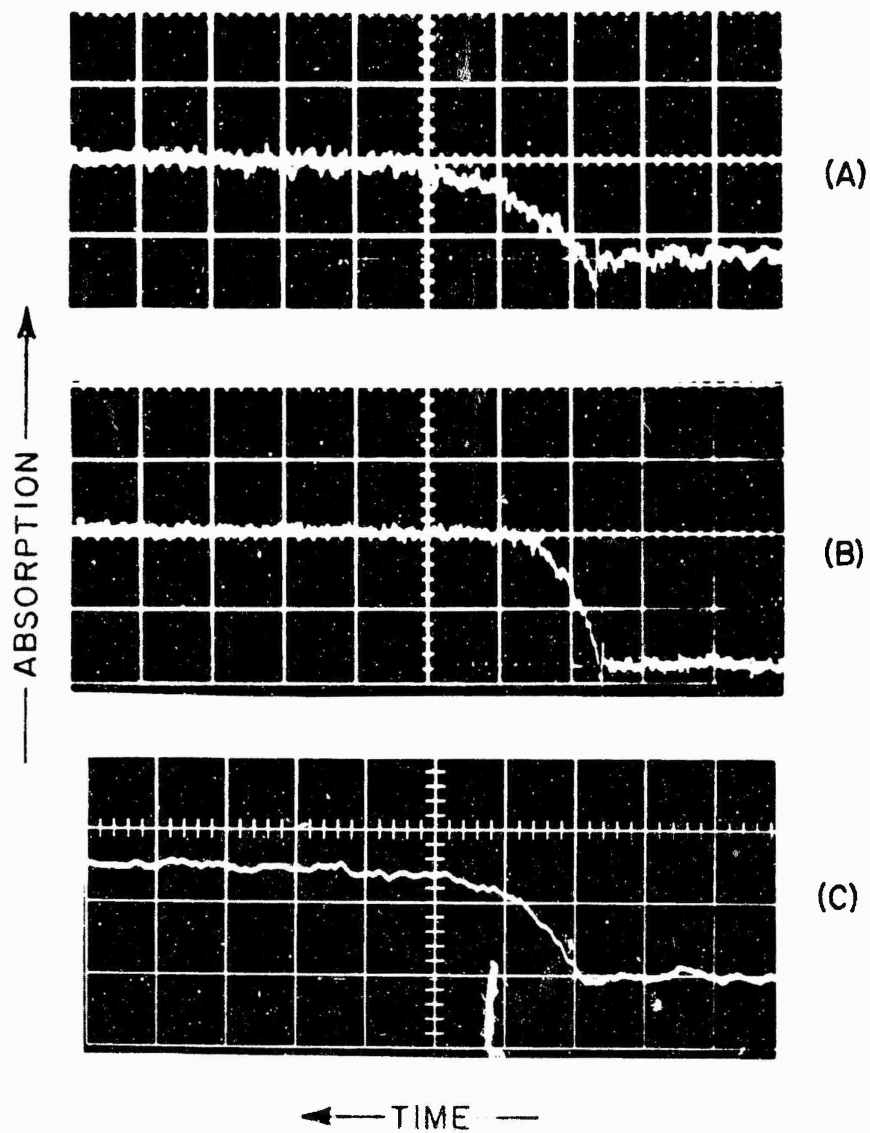
^aconditions for complete dissociation of CF₃I and C₂F₆ at shock front.

TABLE 3

EXAMPLES OF CF₄ SHOCK TUBE EXPERIMENTS

Experiment No.	Shock Velocity (mm/μsec)	^a Shock Temp. (°K)	P ₂₁	Gas Conc'n (mole/cm ³)10 ⁵	Apparent Rate Constant (k ₄ , cm ³ /mole sec)
1:100 CF ₄ - Argon Data					
11	1.559	2410	3.75	1.82	7.96 x 10 ⁷
12	1.623	2590	3.78	1.63	3.32 x 10 ⁸
13	1.643	2640	3.795	1.42	5.61 x 10 ⁸
14	1.670	2720	3.808	0.518	1.04 x 10 ⁹
15	1.715	2850	3.83	0.422	1.89 x 10 ⁹
^a 16	1.795	2970	4.05	1.09	4.70 x 10 ⁹
2:100 CF ₄ - Argon Data					
17	1.507	2260	3.81	1.84	2.91 x 10 ⁷
18	1.544	2350	3.845	1.76	6.12 x 10 ⁷
19	1.591	2460	3.87	1.67	1.34 x 10 ⁸
20	1.623	2550	3.89	1.57	3.63 x 10 ⁸
21	1.66	2650	3.91	1.39	8.20 x 10 ⁸
CF ₄ Data					
22	2.015	2145	19.1	0.515	5.10 x 10 ⁶
23	2.075	2248	19.4	0.521	2.42 x 10 ⁷

^aRate constant evaluated at 40 percent decomposition.



27-3651

Figure 1 Difluoromethylene ultraviolet light absorption behind shock waves into

(a) 1:100 $\text{CF}_3\text{I}-\text{Ar}$, shock veloc. = 1.377 mm/ μ sec, Temp = 1984° K

(b) 1:100 $\text{C}_2\text{F}_6-\text{Ar}$, shock veloc. = 1.456 mm/ μ sec, Temp = 2107° K

(c) 1:100 CF_4-Ar , shock veloc. = 1.782 mm/ μ sec, Temp = 3050° K

at 4 cm Hg initial pressure. Oscillogram writing = 20 μ sec/cm

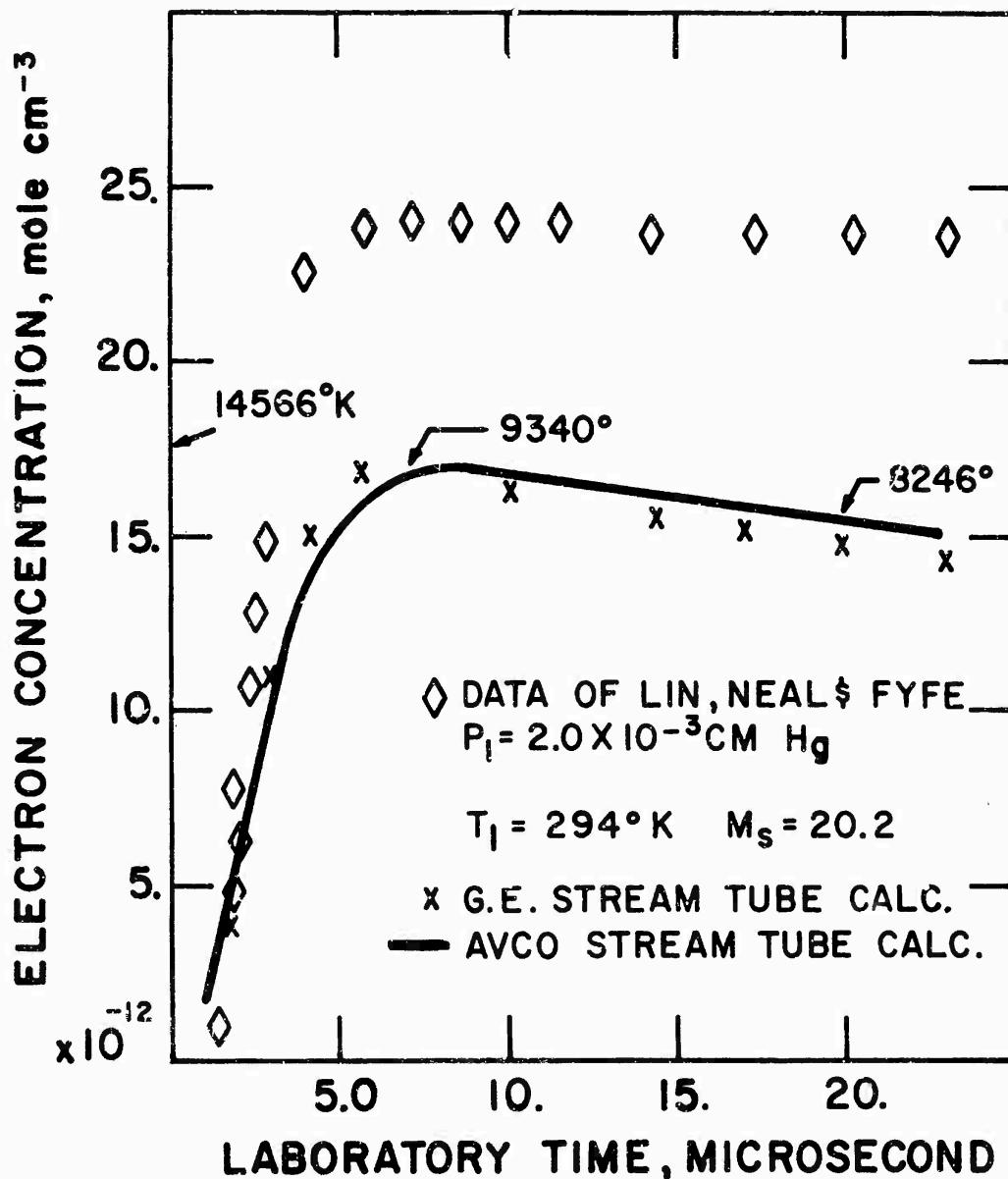
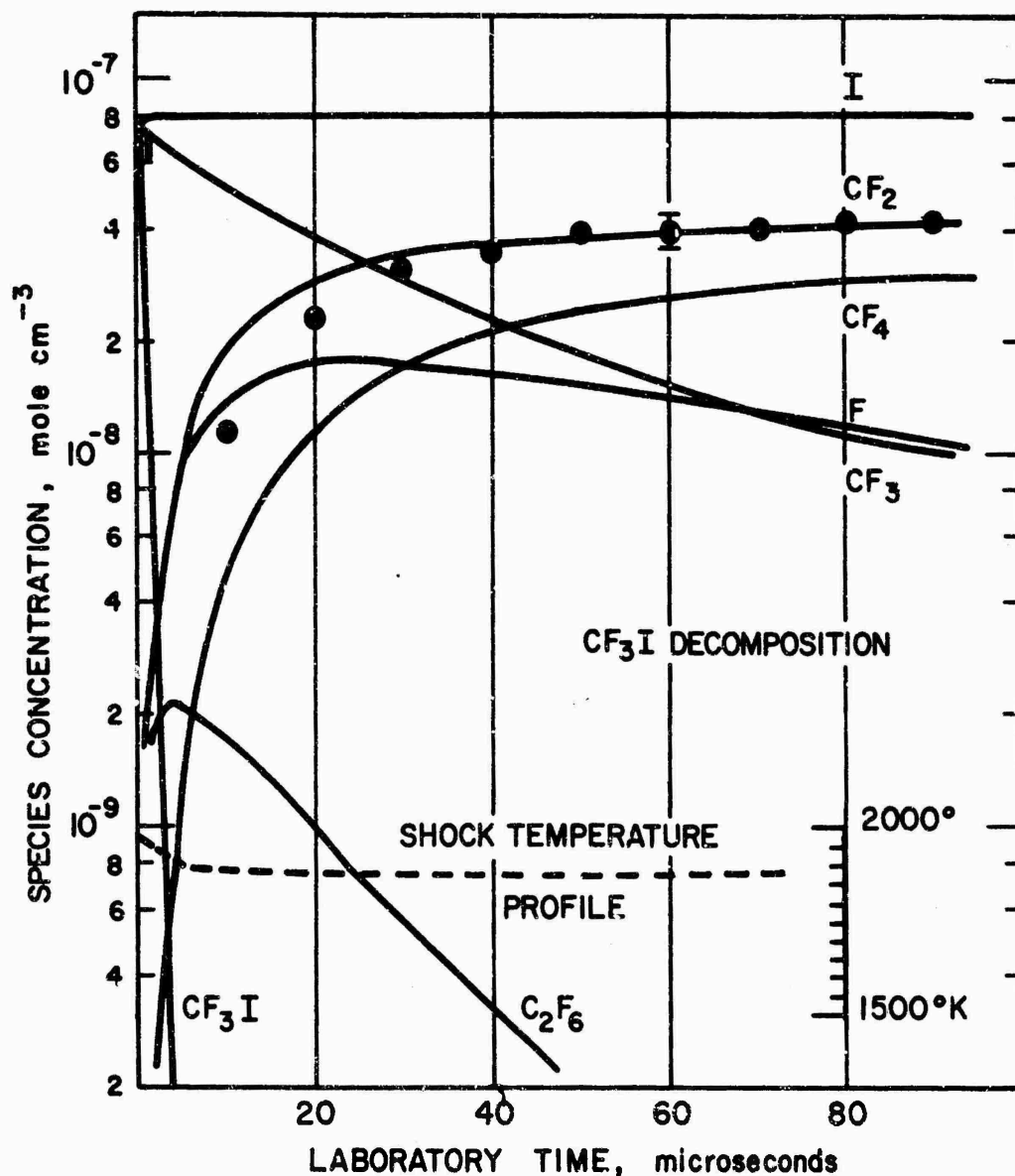
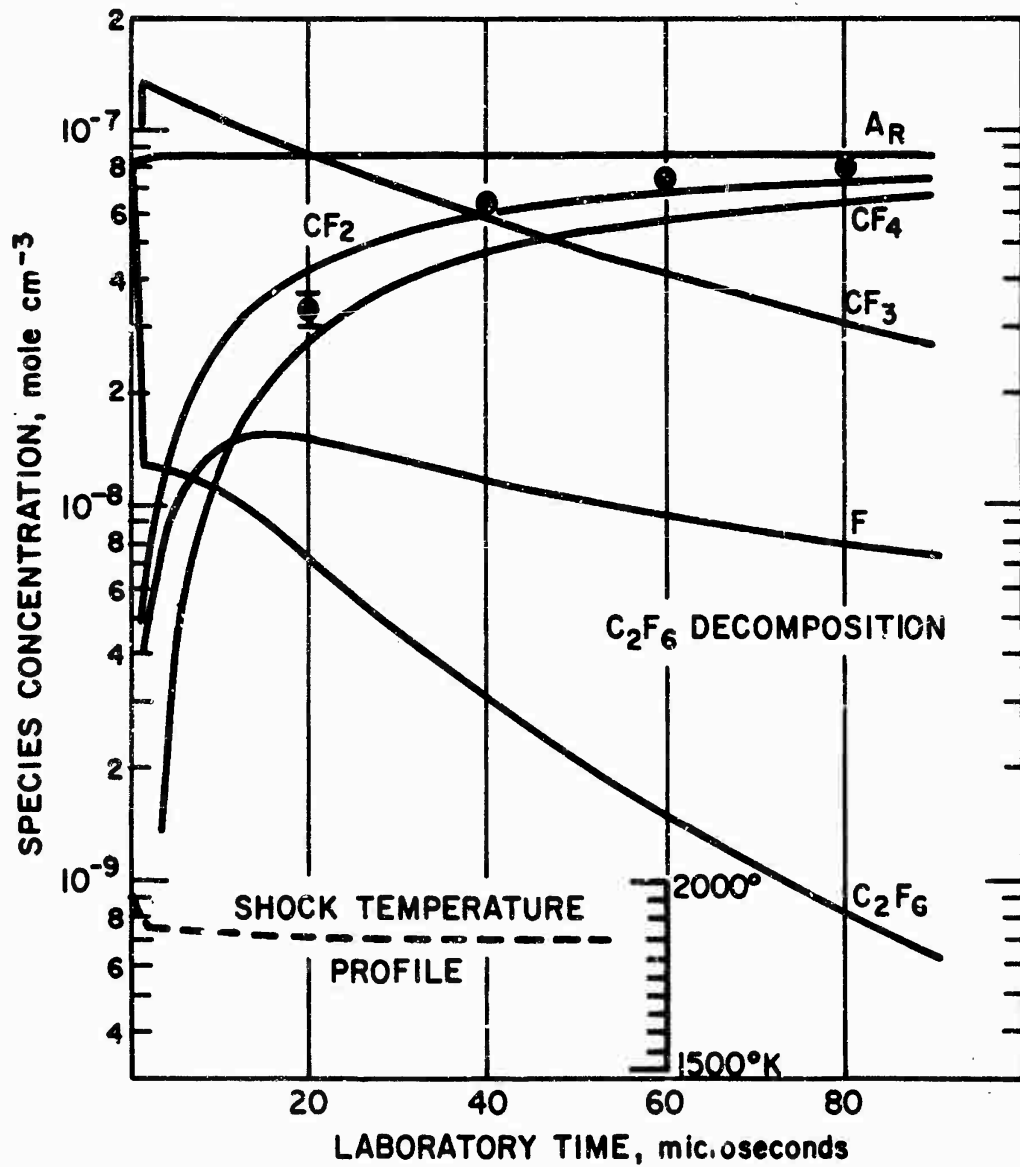


Figure 2 Numerical Check of Nonequilibrium Shock-Tube Program with Airchemistry Stream-Tube Calculation. \diamond , ["Rate of Ionization Behind Shock Waves in Air. I. Experimental Results," Avco/Everett Research Rept. 105, (September, 1960)].



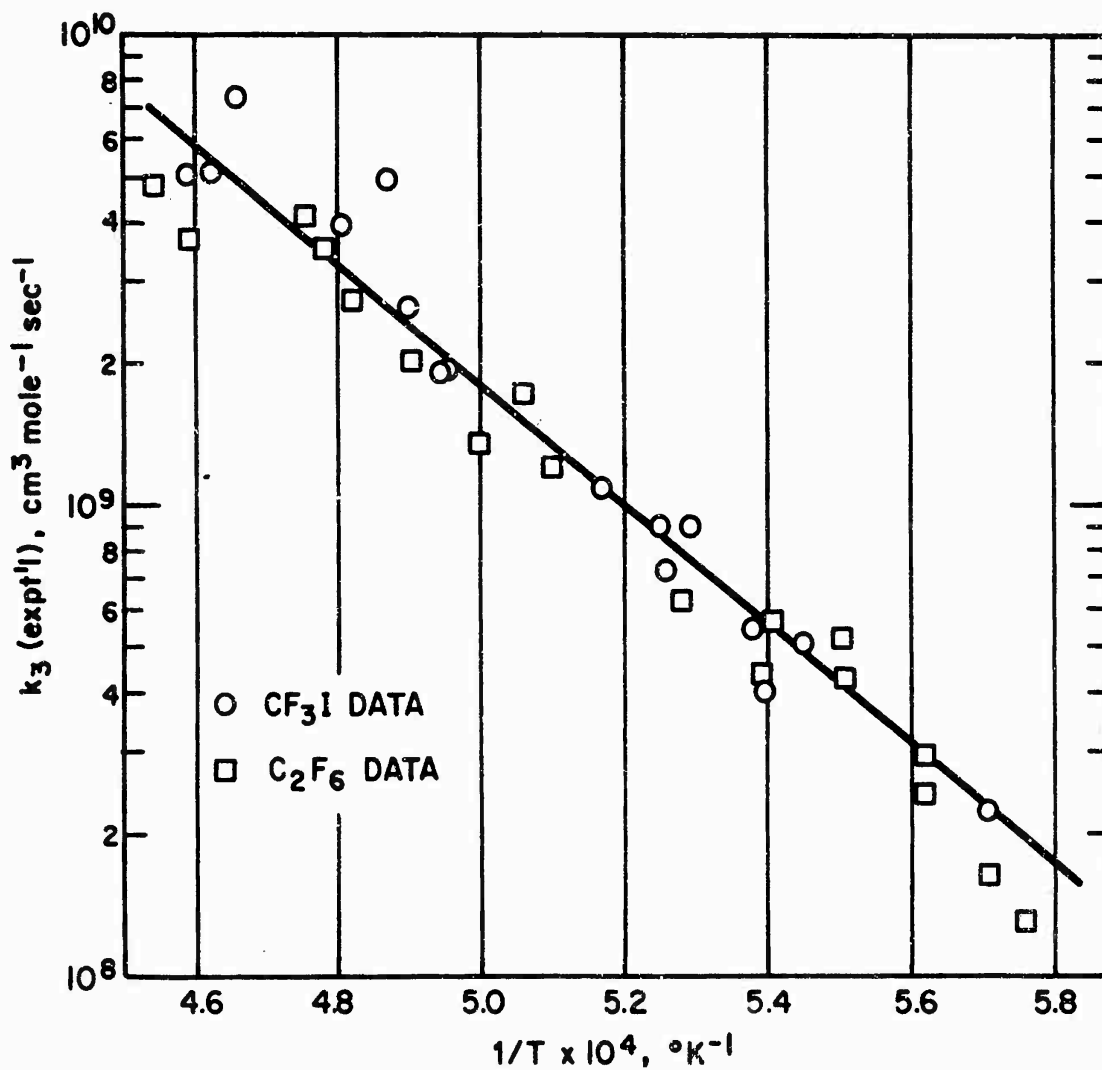
27-3644

Figure 3 Chemical kinetics shock-tube calculation for decomposition of 1:100 CF_3I -Argon gas mixture (Experiment No. 2). \odot , spectroscopic measurements of CF_2 concentration. Error flag reflects uncertainty in absorption coefficient used in data reduction. Argon curve is (100) I.



27-3645

Figure 4 Chemical kinetics shock-tube calculation for decomposition of 1:100 C₂F₆ - Argon gas mixture (Experiment No. 7). ○, spectroscopic measurements of CF₂ concentration.

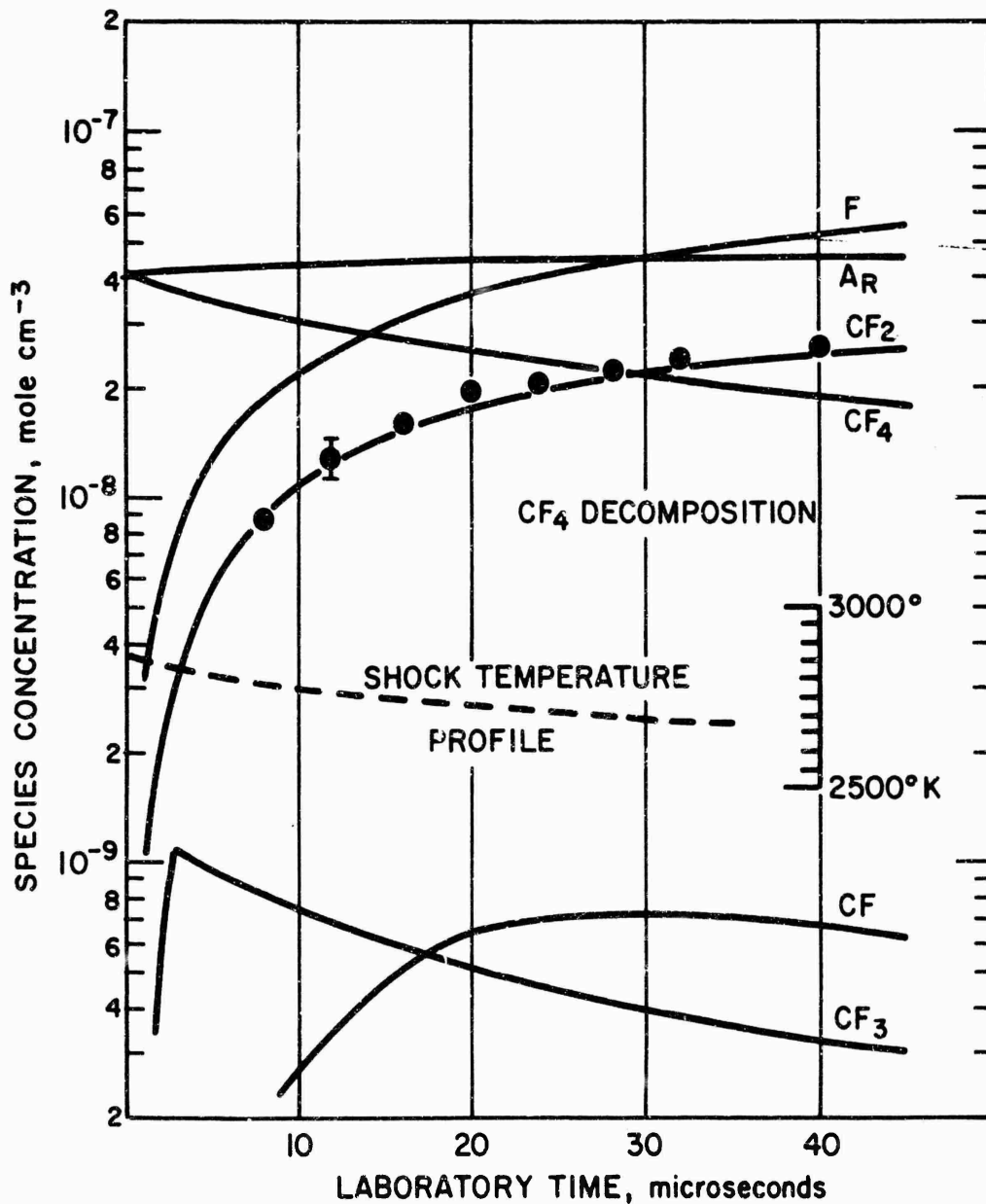


27-3647

Figure 5 Experimental rate constant for CF₃ dissociation. Solid line is the function

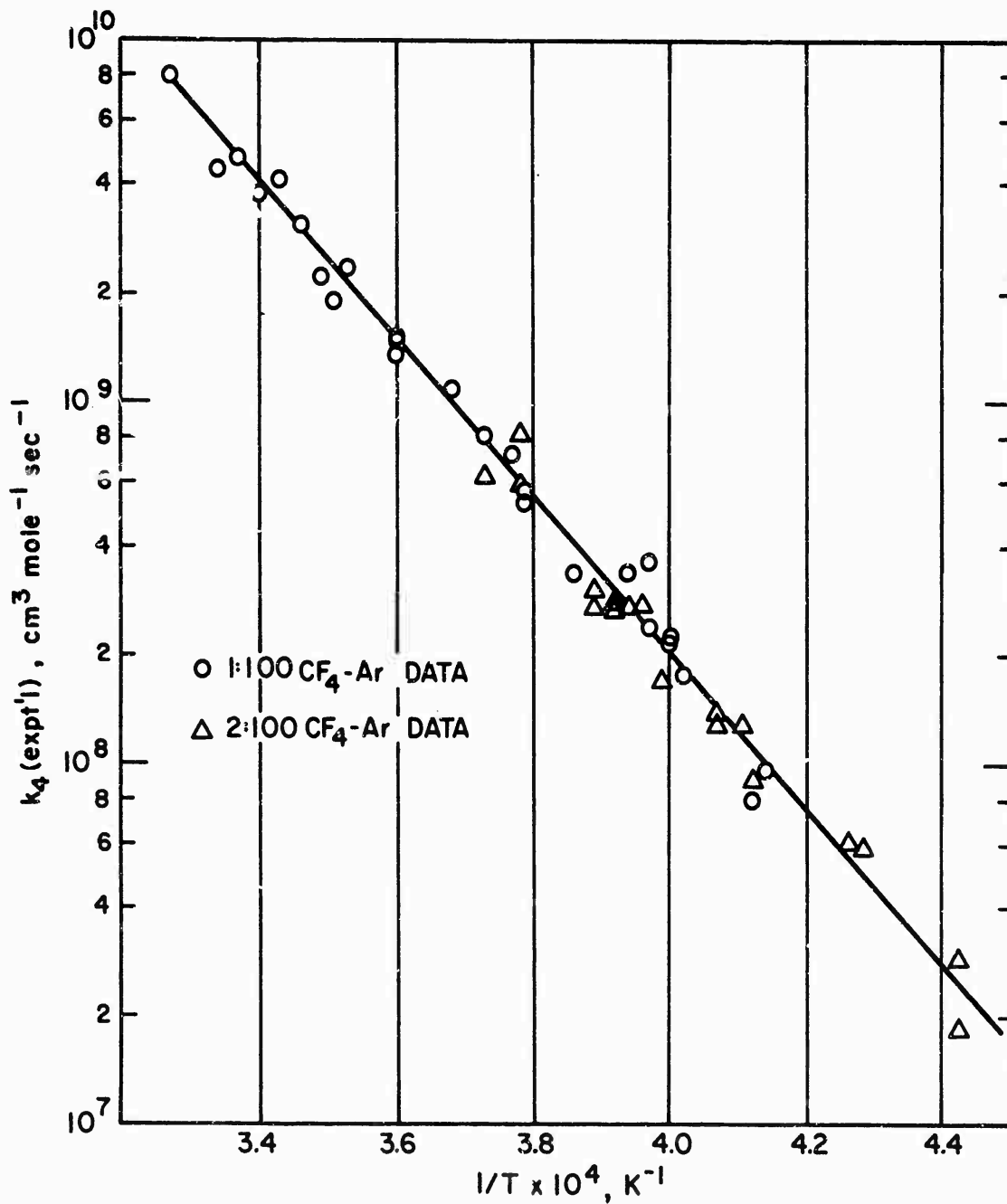
$$1.57 \times 10^{49} T^{-9.04} \exp(-92254/RT)$$

cm³ mole⁻¹ sec⁻¹ from least squares fit of data.



27-3648

Figure 6 Chemical kinetics shock-tube calculation for decomposition of 1:100 CF₄ - Argon gas mixture (Experiment No. 15). ○, spectroscopic measurements of CF₂ concentration.

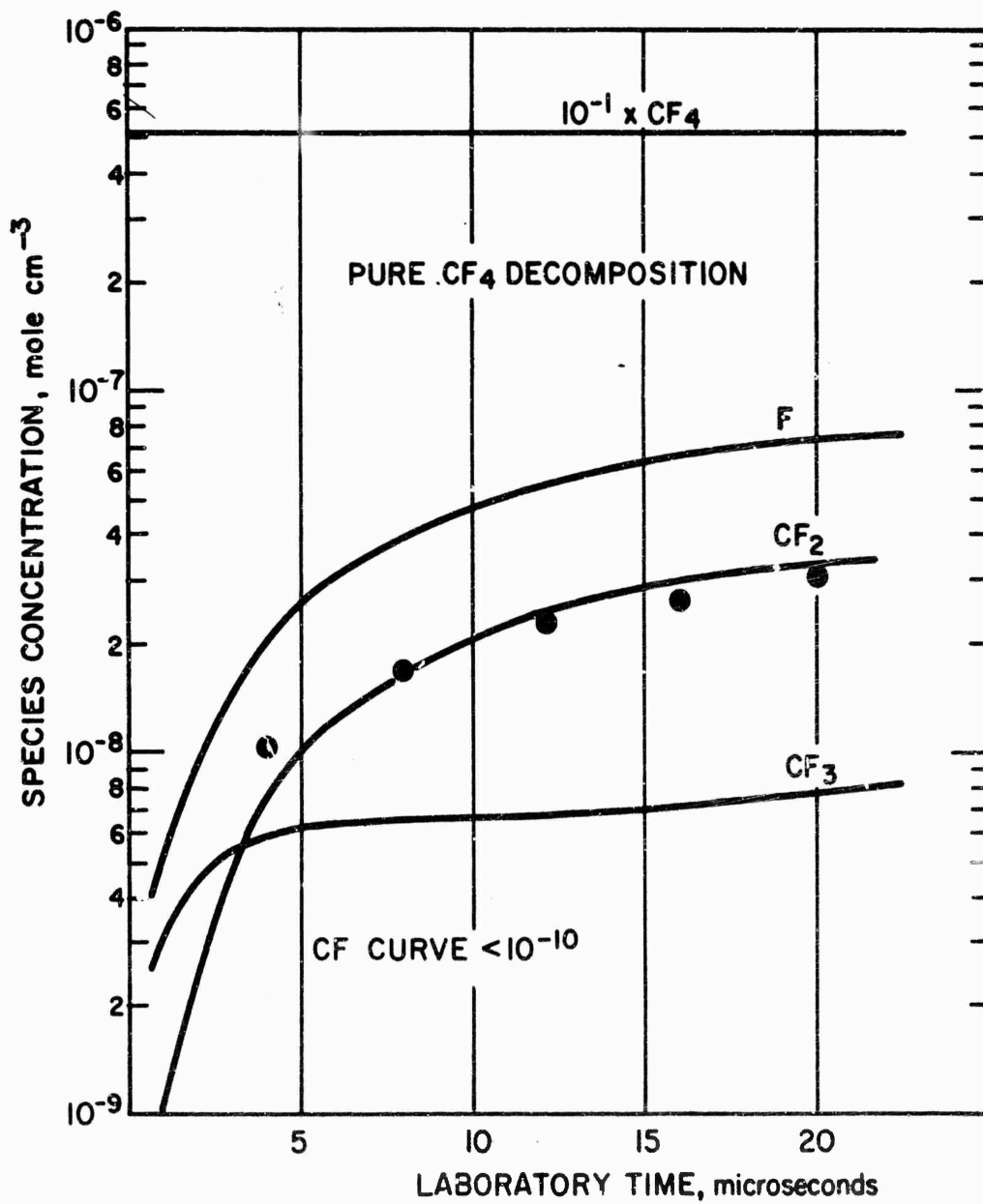


27-3649

Figure 7 Experimental rate constant for CF_4 dissociation. Solid line is the function

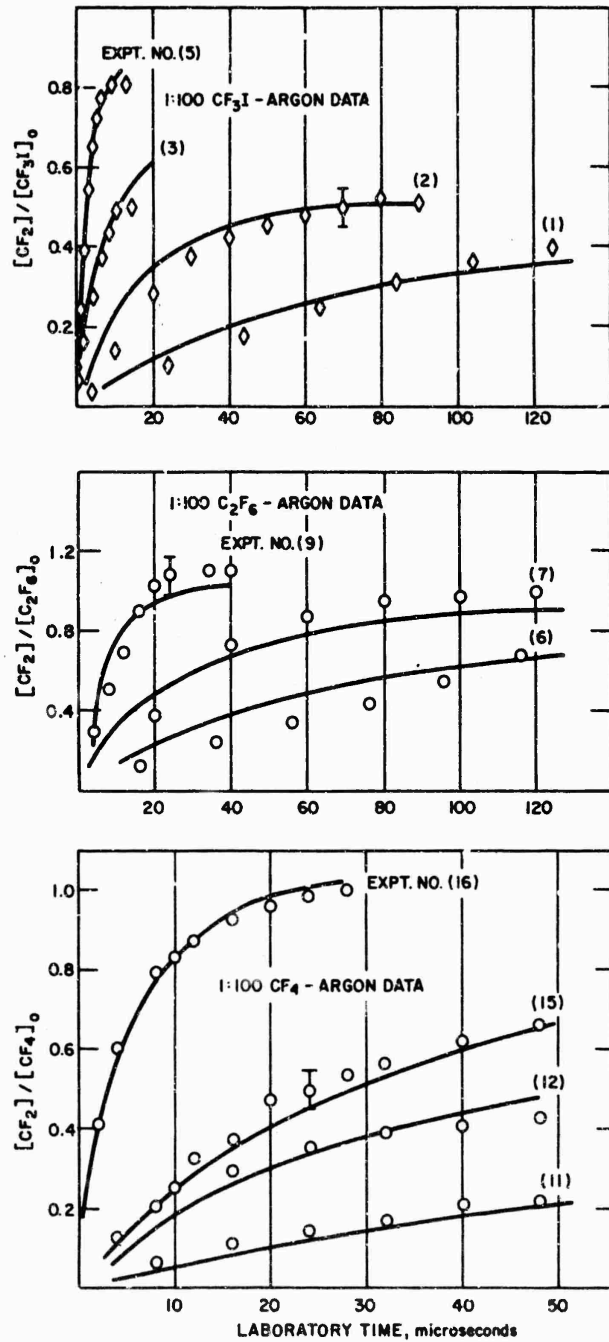
$$6.15 \times 10^{34} T^{-4.64} \exp(-122421/RT)$$

$\text{cm}^3 \text{mole}^{-1} \text{sec}^{-1}$ from least squares fit of data.



27-3646

Figure 8 Chemical kinetics shock-tube calculation for decomposition of pure CF₄ (Experiment No. 22). ⊙, spectroscopic measurements of CF₂ concentration in reaction mixture.



27-3650

Figure 9 Kinetic profiles of CF_2 in shock heated fluorocarbon-argon gas mixtures. Curves are calculated by the nonequilibrium shock-tube program. Symbols are spectroscopic measurements. Subscript 0 denotes reactant concentration initially behind shock wave.